

## Refractive Focusing of Interstellar Clouds and Intraday Polarization Angle Swings

Shan-Jie Qian<sup>1</sup>, T. P. Krichbaum<sup>2</sup>, Long Gao<sup>1</sup>, Xi-Zhen Zhang<sup>1</sup>, A. Witzel<sup>2</sup> and J. A. Zensus<sup>2</sup>

<sup>1</sup> National Astronomical Observatories, Chinese Academy of Sciences, Beijing 100012; [rqsj@bao.ac.cn](mailto:rqsj@bao.ac.cn)

<sup>2</sup> Max-Planck-Institut für Radioastronomie, Auf dem Hügel 69, 53121 Bonn, Germany

Received 2006 June 10; accepted 2006 August 9

**Abstract** Intraday variations of compact extragalactic radio sources in flux density and polarization are generally interpreted in terms of refractive scintillation from the continuous interstellar medium of our Galaxy. However, continuous polarization angle swings of  $\sim 180^\circ$  (for example, the one observed in the QSO 0917+624) could not be interpreted in this way. Qian et al. have shown that the polarization angle swing observed in the QSO 1150+812 can be explained in terms of focusing–defocusing effect by an interstellar cloud, which occults two closely-placed polarized components. Here we further show that the polarization angle swing event observed in the QSO 0917+624 can also be explained in this way. We also found evidence for the cloud eclipsing a non-polarized (core) component during a short period outside the swing. A particular (and specific) plasma-lens model is proposed to model-fit the polarization swing event of 0917+624. Some physical parameters related to the plasma-lens and the source components are estimated. The brightness temperatures of the two lensed components are estimated to be  $\sim 1.6 \times 10^{13}$  K. Thus bulk relativistic motion with a Lorentz factor less than  $\sim 20$  may be sufficient to avoid the inverse - Compton catastrophe.

**Key words:** radio continuum: galaxies — polarization: intraday variability — scattering: refractive focusing — quasars: Individual: QSO 0917+624

### 1 INTRODUCTION

For the study of intraday variability (IDV, hereafter) of compact extragalactic flat-spectrum radio sources (Witzel 1992; Wagner & Witzel 1995; Qian et al. 1991, 2001a, 2002), polarization properties are important. Generally, the variability amplitude observed in polarization is significantly larger than that observed in intensity, while the time scale observed in polarization is much shorter. The relationship between the intraday variations of polarization and intensity in a broad-band (e.g. 2 – 20 cm) may be an important clue to the origin of these variations (e.g. Qian et al. 2002). For explaining the intraday polarization variations both intrinsic models (Qian et al. 1991, 2002; Gopal-Krishna & Wiita 1992; Marscher et al. 1992) and scintillation models (Qian 1994a,b; Rickett et al. 1995, 2002; Simonetti 1991; Qian et al. 2001a, b) have been suggested. Among the IDVs, rapid polarization angle swing events of  $\sim 180^\circ$  with timescale of  $\lesssim 1$  day are particularly interesting. They may imply some regularity in the responsible physical process and may be useful to our understanding of their origin.

However, polarization angle swing events have not been interpreted in the framework of refractive scintillation from the continuous interstellar medium, although the IDVs in total flux density and polarized flux density can be well explained in terms of refractive scintillation. For example, Rickett et al. (1995) proposed a scintillation model to explain the intraday variations of intensity and polarization observed in the QSO 0917+624 and clearly claimed that the event of polarization angle swing of  $\sim 180^\circ$  could not be interpreted, suggesting it to be possibly due to low-level intrinsic activity.

Simonetti (1991) attempted to interpret the polarization angle swing event observed in 0917+ 624 in terms of refractive focusing–defocusing effect by an interstellar shock passing in front of the source, however, this model can only explain a polarization angle ‘jump’ of  $\sim 180^\circ$ , and not the continuous swing as observed in 0917+624. Simonetti (1991) suggested that in order to explain the observed polarization position angles near the midway of the swing, some other mechanism (intrinsic or focusing by another cloud) is needed.

Refractive focusing–defocusing effect by interstellar clouds have been applied to interpret the rapid variations of flux density in compact extragalactic sources at centimeter wavelengths with timescales in the range from a few weeks to months (usually called ‘extremely scattering events’, for example: Fiedler et al. 1987; Clegg et al. 1988, 1996; Pohl et al. 1995). The basic effect of refractive focusing–defocusing is to produce light curves eclipsed by the clouds. These eclipsed light curves (in some cases with a few peaks within the troughs) have been observed in several sources (for example, 0954+658: Fiedler et al. 1987; 0528+134: Pohl et al. 1995; 1741–038: Clegg et al. 1988).

Wambsganss et al. (1989) have shown that focusing–defocusing effects by an ensemble of interstellar clouds can explain intraday variability in total flux density, but intraday variability in polarization was not discussed in this way.

Qian et al. (2006) was first to investigate the conditions under which intraday polarization angle swing of  $\sim 180^\circ$  could arise from refractive focusing–defocusing effects by interstellar clouds and provided a plausible explanation for the polarization angle swing event observed in the QSO 1150+812 (Kochenov & Gabuzda 1999). Here in this paper we will show that the polarization angle swing event of 0917+624 can also be interpreted in the same way, further indicating the significance of the focusing–defocusing effects by interstellar clouds in the production of polarization IDVs.

## 2 RECAPITULATION OF THE SWING EVENT OF 0917+624

We first briefly recapitulate the properties of the polarization angle swing of  $\sim 180^\circ$  observed in the QSO 0917+624. This event was observed at 6 cm (Quirrenbach et al. 1989) and is shown in Figure 1. The data are taken from Quirrenbach et al. (2000), in which the original data were re-analysed. The event has a time scale of  $\sim 1$  day.

Figure 1 shows some interesting features: the rapid polarization position angle swing of  $\sim 180^\circ$  occurred during the  $\sim 1$  day period (JD24407525.5 – 7526.5). During the rapid position angle swing, the polarized flux density reached a minimum near the midway of the swing with two peaks at its either side. The full amplitude is only  $\sim 5$  mJy. This behaviour of polarized flux density is not different from the behaviour in the time interval between 7524.0 – 7525.5, when the position angle is nearly constant. The total flux density variation is more irregular, having a peak near 7527.5 and a flat minimum at  $\sim 7625.75$ .

It seems very difficult to explain all the properties together (including the polarization angle swing and the variations in total and polarized flux density). For example, Rickett et al. (1995) have reasonably well interpreted the properties in terms of scintillation from a continuous interstellar medium, but admitted unable to explain the polarization angle swing. Similarly, the refractive focusing model proposed by Simonetti (1991), though suggestive, could only explain a ‘jump’ in the polarization angle, and is unable to interpret the continuous polarization angle swing like that observed in 0917+624.

Moreover, since the compact source of 0917+624 has a core–jet structure with multi-components, the range in which the polarization angle swings could not be simply related to those of the VLBI polarized components (Standke et al. 1996; Krichbaum et al. 2002). Thus in the following section we will follow the approach proposed by Qian et al. (2006) and consider a four–component model (three polarized and one non-polarized), the parameters of which are chosen through trial calculations to see in what conditions a continuous polarization angle swing can be produced through vector combination of the polarizations of the components. Our work resulted in the conclusion that the polarization angle swing could be due to the occultation of two polarization components through the focusing–defocusing effect of an interstellar cloud.

## 3 MODEL–FITTING OF POLARIZATION ANGLE SWING

As shown in Qian et al. (2006), in order to explain the *continuous* polarization angle swing of  $\sim 180^\circ$  three polarized components were needed. Thus we follow Qian et al. (2006) and consider a four-component model with three polarized and one non-polarized (probably the compact core). We take component-1 and

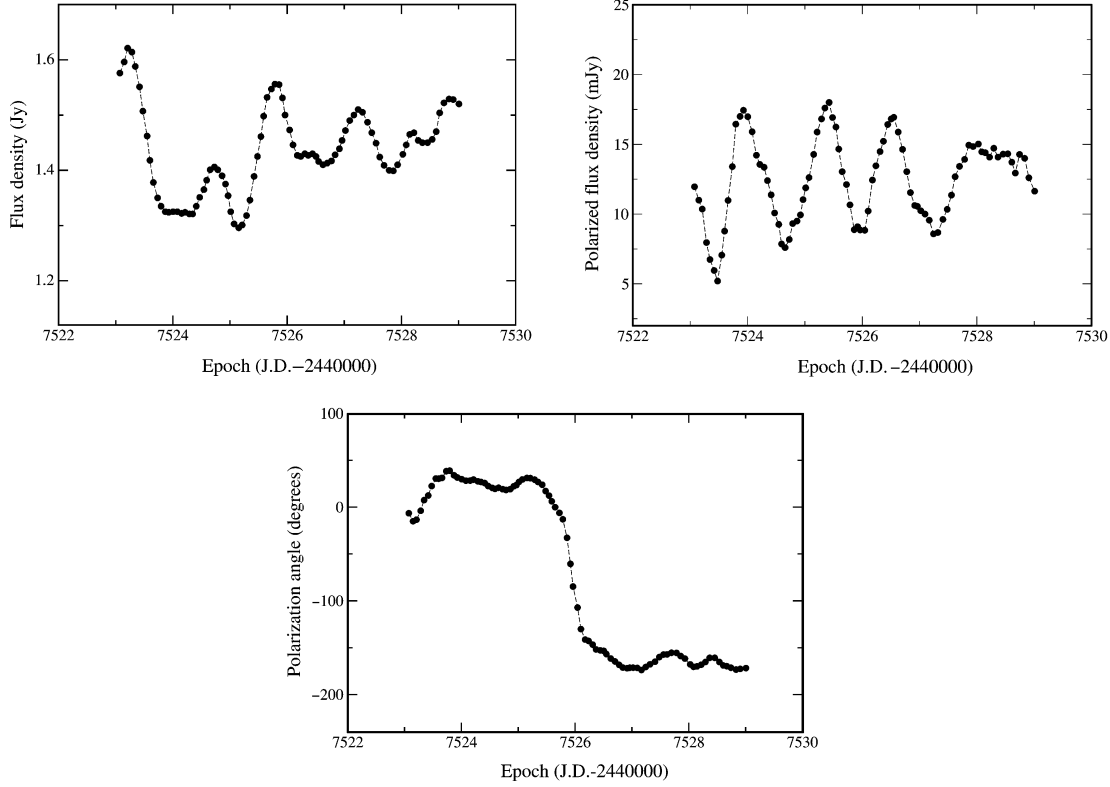


**Fig. 1** Polarization position angle swing event observed in 0917+624 at 6 cm: the light curves of total flux density (upper left), polarized flux density (upper right) and polarization position angle.

component-2 to be variable in polarized flux density due to interstellar scintillation, and component-3 to be a stable polarized component. Component-4 is assumed to be non-polarized and only varies in intensity. All the position angles of the four components are assumed to be constant. Thus the observed polarization should be equal to the vector combination of the three polarized components. We can write the equations for the Stokes parameters as:

$$S_{p1}(t)\cos 2\chi_1 + S_{p2}(t)\cos 2\chi_2 = S_p(t)\cos 2\chi(t) - S_{p3}\cos 2\chi_3, \quad (1)$$

$$S_{p1}(t)\sin 2\chi_1 + S_{p2}(t)\sin 2\chi_2 = S_p(t)\sin 2\chi(t) - S_{p3}\sin 2\chi_3, \quad (2)$$

where  $S_{p1}(t)$ ,  $S_{p2}(t)$  and  $S_{p3}$  are the polarized flux densities of component-1, component-2 and component-3 respectively,  $\chi_1$ ,  $\chi_2$  and  $\chi_3$  are their position angles.  $S_p(t)$  and  $\chi(t)$  are the known, observed polarized flux density and polarization angle.

Equations (1) and (2) contain six unknown parameters, two of which ( $S_{p1}(t)$  and  $S_{p2}(t)$ ) are functions of time. So the equations can not be solved generally and we are not able to obtain any unique solution (multiplicity of solutions is a common problem in the studies of polarization IDVs, see Rickett et al. 2002).

### 3.1 A Particular Model

Following Qian et al.(2006), through trial calculations within certain ranges of values for the four parameters ( $\chi_1, \chi_2, \chi_3, S_{p3}$ ), we have searched particular solutions which can reproduce the observed polarization angle swing and satisfy the constraint that the polarized flux densities  $S_{p1}(t)$ ,  $S_{p2}(t)$  and  $S_{p3}$  are always *positive*. One of the particular solutions is shown in Figure 2 for  $S_{p1}(t)$  and  $S_{p2}(t)$  with  $\chi_1=+45^\circ$ ,  $\chi_2=-60^\circ$ ,  $\chi_3=0^\circ$  and  $S_{p3}=20$  mJy.

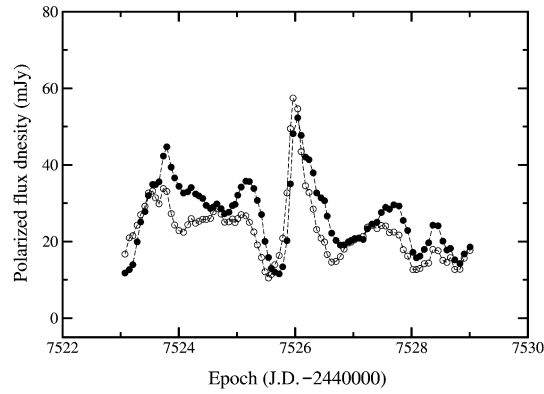


**Fig. 2** Light curves of the polarized flux density of component-1 and component-2. The chosen parameters are:  $\chi_1=+45^\circ$ ,  $\chi_2=-60^\circ$ ,  $\chi_3=0^\circ$  and  $S_{p3}=20$  mJy. Filled circles –  $S_{p1}(t)$ , unfilled circles –  $S_{p2}(t)$ .

It can be seen that the light curves  $S_{p1}(t)$  and  $S_{p2}(t)$  are very similar, both showing a sharp decrease and then a rapid rise during the swing period ( $\sim 7525.25 - 7526.25$ ). We found that all the solutions of the equations have this characteristic, thus the solution shown in Figure 2 is representative. Moreover, the light curves of  $S_{p1}(t)$  and  $S_{p2}(t)$  during the swing period are quite similar to the patterns usually seen in the extreme scattering events (ESEs) (or focusing–defocusing events; Fiedler et al. 1987, 1994 and Clegg et al. 1996, 1998), but with a much shorter time scale of  $\sim 1$  day. The two light curves have a minimum at  $\sim 7525.55$  and  $7525.65$ , respectively, and both decrease from normal level ( $\sim 30$  mJy) to  $\sim 10$  mJy and then sharply increase up to  $\sim 60$  mJy. The light curve of the component-2 leads that of the component-1 by about 0.1 days. The cross correlation coefficient between the two light curves is about 0.99, almost a perfect correlation. This indicates that the observed polarization angle swing event observed in 0917+624 can be interpreted as to be a simultaneous focusing event of two polarized components (see below and Qian et al. 2006).

### 3.2 Light Curves of Flux Density and Correlation

The light curves of the flux density of the two variable components can not be determined, because we do not know their polarization degrees. VLBI polarization observations (for example, Gabuzda & Cawthorne 2000; Gabuzda et al. 1996) show that VLBI components can have very different percentage polarization, from  $\lesssim 2\%$  (core) to  $\sim 10\% - 60\%$  (jet components). We will take a specific value of 20% for the polarization degree of both component-1 and component-2. Then we have the light curves of the summed flux density of the two components (left panel) and the remaining part of the flux density (the summed flux density of component-3 and component-4) shown in Figure 3.

It is clear from Figure 3 that the light curve of the summed flux density of component-1 and component-2 shows a similar pattern of the focusing process (like that in Fig. 2) with an amplitude of variation of  $\sim 0.4$  Jy. It is worth to point out that during the period (7524.7–7526.0) the light curve of the summed flux density of component-3 and component-4 (right panel in Fig. 3) shows a pattern closely similar to that of the summed flux density of component-1 and component-2 during the swing period (left panel in Fig. 3). We chose part of the former light curve (epoch 7524.8–7526.3) and part of the latter light curve (epoch 7525.3–7526.7) to make a correlation, and obtained a correlation coefficient of  $\sim 0.8$ . Although this is not strong evidence, it might imply that the flux density variation of the non-polarized core (component-4, the dominated flux density component) is also affected by the focusing–defocusing effect of the cloud, and in the studies of IDVs the effects from the continuous medium and individual clouds both should be taken into account (in other words, the effects from individual clouds may dominate in some cases). However, in this paper we will not discuss the variations outside the swing period when some combination of scintillation from the continuous medium and clouds may be at work. The problem becomes complex when we have to take into account both the effects.

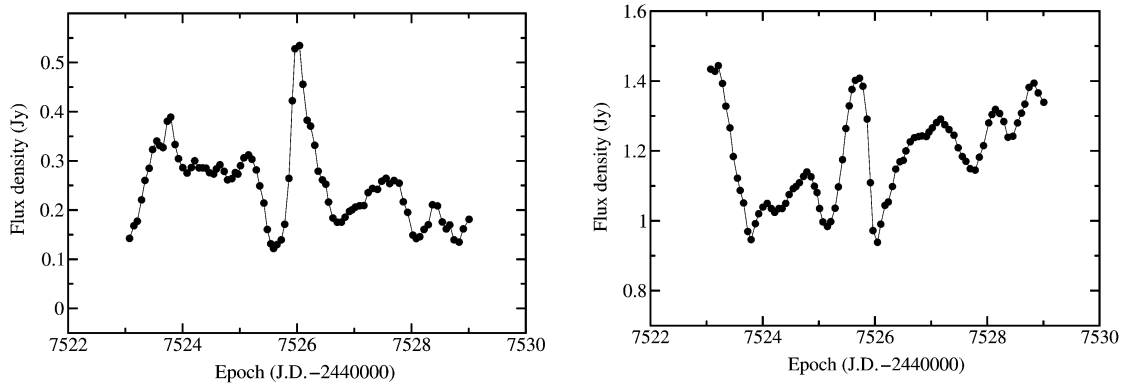


**Fig. 3** For an assumed polarization degrees of component-1 and component-2 of 20%, the light curves of the summed flux density of component-1 and component-2 (left panel), and the summed flux density of component-3 and component-4 (right panel).

In the following section we will discuss a mechanism which can reproduce the light curves of  $S_{p1}(t)$  and  $S_{p2}(t)$  during the swing period ( $\sim 7525.0$ – $7526.5$ ) shown in Figure 2.

## 4 REFRACTIVE FOCUSING BY A PLASMA-LENS

### 4.1 Introduction

Refractive focusing–defocusing effects caused by interstellar clouds have been invoked to interpret the so-called ‘extreme scattering events’ observed at cm-dm bands with timescales of weeks and months (0956+658: Fiedler et al. 1994, 1987; 1741–038: Clegg et al. 1988, 1996; 0528+134: Pohl et al. 1995). The intensity light curves of ESEs were observed to have a characteristic pattern: a deep extended minimum bracketed by two bumps, and in some cases, with a few peaks occurring within the extended minimum at high frequencies. A ‘classical’ example is that observed in the QSO 0954+658, its observed properties were discussed in detail by Fiedler et al. (1987). The extended minimum observed at 2.23 GHz was interpreted as due to refractive defocusing by a cloud (or an ‘occultation event’) and the multiple spikes observed at 8 GHz as due to refractive focusing and formation of caustics (or multiple images). They also estimated some parameters related to the interstellar clouds (size of the clouds, electron column density, distance to the observer) and the compact source (angular size, flux density). Clegg et al. (1996) have studied an ESE observed in 1741–038 with a timescale of  $\sim 0.4$  years at 2.23 GHz (the long-term multi-frequency intensity light curves of the source have been analyzed by Qian et al. 1995). The behavior of this event is different from that observed in 0954+658 in that the 8.1 GHz light curve did not show strong spikes, implying a weak refractive focusing. In addition, Clegg et al. (1996, 1998) have proposed a plasma-lens model to interpret the properties of the ESEs observed in both 0954+658 and 1741–038, on the basis of the geometric optics of refractive focusing process. They discussed the geometric optics of refraction of an extragalactic radio source by an interstellar cloud as a plasma lens. The general properties are: around the axis of the plasma-lens, defocusing of the source intensity forms an extended minimum in the light curves, and at both sides focusing form sharp caustic spikes (if the source is very compact) or peaks (or bumps, if the source size is comparable to, or larger than that of the lens), bracketing the minimum. At higher frequencies caustic spikes can be formed even within the extended minimum. The information can lead to estimation of the properties of the medium and the compact source component.

As was shown above in Section 2, during the swing period the light curves of the polarized component-1 and component-2 are very similar to those of ESEs observed in 0956+658 and 1471–038 (a pattern consists of a deep minimum and a peak), so we will apply the plasma-lens model proposed by Clegg et al. (1996, 1998) to interpret our results.

## 4.2 Plasma-Lens Model

The one-dimensional Gaussian plasma-lens model proposed by Clegg et al.(1998) contains two independent dimensionless parameters  $\alpha$  and  $\beta_s$ ,

$$\alpha = \left( \frac{\sqrt{\lambda D}}{a} \right)^2 \left( \frac{\lambda r_e N_0}{\pi} \right), \quad (3)$$

and

$$\beta_s = \theta_s / \theta_l. \quad (4)$$

Numerically,

$$\alpha = 3.8 \times 10^{-3} \left( \frac{\lambda}{\text{cm}} \right)^2 \left( \frac{N_0}{\text{cm}^{-3} \text{pc}} \right) \left( \frac{D}{\text{pc}} \right) \left( \frac{a}{\text{AU}} \right)^{-2}. \quad (5)$$

Here  $D$ – distance of the plasma-lens to the observer,  $\lambda$  – wavelength,  $a$  – linear size of the plasma-lens,  $N_0$  – the peak column free-electron density. The distribution of electron density is assumed to be Gaussian:  $N_e(x) = N_0 \exp[-(x/a)^2]$  (coordinate  $x$  denotes position transverse to the line of sight),  $\theta_s$ – angular size of the source,  $\theta_l$ – angular size of the lens as seen by the observer. It can be seen that the parameter  $\alpha$  is a function of the wavelength of observation, the free-electron column density through the lens, the lens - observer distance and the diameter of the lens transverse to the line of sight. The refractive properties of the lens are specified completely by a dimensionless parameter  $\alpha$ . However, the pattern of ESE light curves of the source which is lensed by the plasma-lens depends on the dimensionless parameter  $\alpha$  and the relative size of the source and the lens as seen by the observer. The time interval  $\Delta t$  between the inner peaks (or caustics) is a measure for the time scale of focusing events. It is related to the linear size of the lens and the relative velocity  $v$  between the lens and the observer:

$$\Delta t \approx 4.3a/v. \quad (6)$$

Here we should point out that, for the case studied here,  $\alpha$  is less than the minimal value which can form caustics, the value of the coefficient may be slightly less than 4.3.

## 4.3 Model-Fitting

Following the treatment of the ESEs by geometric optics given by Clegg et al. (1998), the ray-path equation for an extended source is solved to obtain the modelled light curves. We assume that the source brightness distribution has a Gaussian form ( $-\theta_s/2 \leq \theta \leq \theta_s/2$ ):

$$B(\theta) \propto \exp\left[-\left(\frac{\theta}{\theta_s}\right)^2\right]. \quad (7)$$

Each ray incident on the lens at position  $x$  is refracted through a refracting angle and strikes at the position  $x'$  on the observer's plane. The ray-path equation gives the relation:

$$u[1 + \alpha \exp(-u^2)] - (u' + \beta) = 0, \quad (8)$$

where  $\beta = \theta/\theta_s$ ,  $u = x/a$  and  $u' = x'/a$ . For each ray-path a gain factor is calculated to define the ray strength due to the effects of focusing and defocusing. The light curves will then be obtained by integrating the contributions from all the rays from the extended source. In our case of weak scattering there is no ray crossing (or multiple images), so for each direction there is only one ray-path.

We have used the plasma-lens model to make a fit to the light curves shown in Figure 2. We found that a plasma-lens with  $\alpha=1.5$  and  $\beta_s=0.8$  can produce a reasonable fit to the light curves for both component-1 and component-2. The results are shown in Figures 4 and 5 for the two polarized component -1 and component-2, respectively.

The values of  $\alpha$  and  $\beta_s$  imply that the swing event occurred in weak refractive scattering. The intensity (total and polarized flux density) variations are solely due to focusing and defocusing, no caustics form. The angular size of the polarized components is only slightly smaller than that of the lens, so the light curves have a rounded minimum. It can be seen from Figures 4 and 5 that the fits are good, especially for the

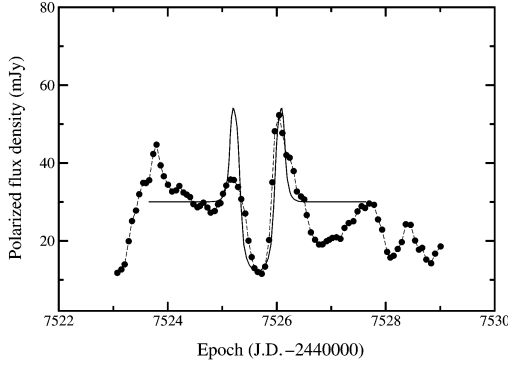


**Fig. 4** Model fitting of the light curve by a plasma-lens model for polarized component-1.  $\alpha=1.5$  and  $\beta_s=0.8$ .

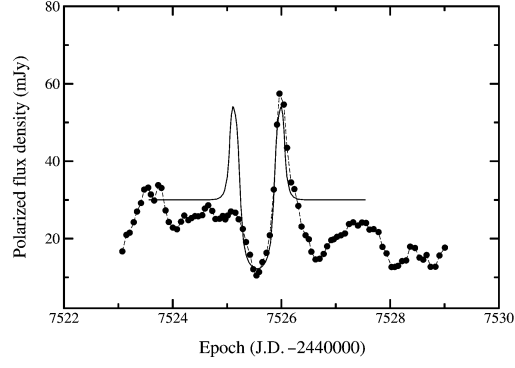


**Fig. 5** Model fitting of the light curve by a plasma-lens model for polarized component-2.  $\alpha=1.5$  and  $\beta_s=0.8$ .

rounded minimum and the peak at  $\sim 7526.1$  for both light curves (the fits obtained here are better than in the case of 1150+812, Qian et al. 2006). The peak at  $\sim 7525.2$  predicted by the model is observed for the component-1, at a reduced amplitude (Fig. 4). For the component-2 the predicted peak at  $\sim 7525.2$  does not appear. Differences between the modelled and observed light curves often appear in model-fitting, like in the cases of 0954+658 and 1741-038 (Clegg et al. 1998) and are usually attributed to be due to substructure within the lens and anisotropic lens shape or lens-grazing of the source.

As we pointed out above, the focusing process of the component-1 lagged behind that of the component-2 only by  $\sim 0.1$  days, and when component-2 was fully ‘occulted’ component-1 was also largely ‘occulted’ (with its polarized flux reduced by  $\sim 70\%$ ), so the two components were almost simultaneously occulted by one cloud. From the model-fitting (Figs. 4 and 5) the two components have very close positions in projection and have similar angular size in the direction of motion of the cloud. Outside the swing period the modelled light curves are constant at a normal level, different from the observed ones. Obviously, this implies that the variations outside the swing period are due to the refractive focusing – defocusing effects from other clouds (Wambsganss et al. 1989) or scintillation from the continuous medium.

In summary, the intraday variations in total flux density and polarization (especially the PA swing event) observed in 0917+624 may be caused by a combination of refractive focusing effects by interstellar clouds and scintillation from the continuous medium, which could dominate at different epochs. This implies that the intraday polarization angle swing of  $\sim 180^\circ$  should be very rare events in the framework of interpretation in terms of refractive focusing effects.

#### 4.4 Estimation of Parameters

On the basis of the plasma-lens model some parameters can be estimated for the properties of the source and the lens. Since we do not know the value of the relative transverse speed between the lens and the observer, we write the following formulae:

$$\frac{a(\text{AU})}{v(\text{km s}^{-1})} \approx 5.6 \times 10^{-6} \Delta t(\text{hour}), \quad (9)$$

$$\frac{\theta_s(\mu\text{as})}{v(\text{km s}^{-1})} \approx 5.6 \frac{\Delta t(\text{hour})}{D(\text{pc})} \beta_s, \quad (10)$$

$$N_0(\text{cm}^{-3}\text{pc}) = 2.6 \times 10^{-10} \alpha \left( \frac{\lambda}{\text{cm}} \right)^{-2} \left( \frac{D}{\text{pc}} \right) \left( \frac{\theta_s}{\mu\text{as}} \right)^2 \beta_s^{-2}, \quad (11)$$

$$n_e(\text{cm}^{-3}) \approx 2.06 \times 10^5 \frac{N_0(\text{cm}^{-3}\text{pc})}{a(\text{AU})}, \quad (12)$$

$$M_l \approx 1.2 \times 10^{-17} \eta \left( \frac{n_e}{\text{cm}^{-3}} \right) \left( \frac{a}{\text{AU}} \right), \quad (13)$$

where  $N_0$  – the peak free-electron column density through the lens along the line of sight,  $n_e$  – the electron density of the lens, and  $M_l$  – mass of the plasma- lens. Here we assume that in the plane normal to the line of sight the cloud is symmetric, having a Gaussian distribution of electron density with size  $a$ .

We point out that source 0917+624 is located in the direction to the Galactic Loop III, and so we assume that the plasma-lens is located in this loop which may be a supernova remnant. The distance of the loop has been estimated to be  $\sim 145$  pc (Hu 1981; Berkhuijsen et al. 1971; Heiles & Jenkins 1976). Thus if we take the velocity to be  $30 - 100$  km s $^{-1}$  (note  $\Delta t = 0.89$  days = 21.4 hours), we obtain the following estimates (in our case the wavelength of observation is 6 cm):  $a = (0.36 - 1.2) \times 10^{-2}$  AU,  $\theta_s = (20 - 66) \mu\text{as}$  (at 6 cm),  $N_0 = (0.98 - 11) \times 10^{-6}$  cm $^{-3}$  pc,  $n_e = (0.56 - 1.9) \times 10^2$  cm $^{-3}$  and  $M_l = (0.031 - 3.9) \times 10^{-21} M_\odot$ .

These values show that the lensed polarized components are very compact and the lens are much smaller than those observed in ESEs. The electron density and the mass of the lens are also much lower than those observed in ESEs in 0954+658 and 1741–038.

The brightness temperatures of the polarized component-1 and component-2 can also be estimated,

$$T_b(\text{K}) = 2 \times 10^{15} (1+z) \left( \frac{S_{\text{obs}}}{\text{Jy}} \right) \left( \frac{\lambda_{\text{obs}}}{\text{cm}} \right)^2 \left( \frac{\theta_s}{\mu\text{as}} \right)^{-2}. \quad (14)$$

If we take  $S=0.15$  Jy (corresponding to polarization degree of 20%, at 6 cm), and  $\theta_s=40 \mu\text{as}$  ( $v = 60$  km s $^{-1}$ ), then we obtain  $T_b = 1.6 \times 10^{13}$  K. Thus, relativistic motion with Lorentz factor  $\lesssim 20$  is sufficient to bring down the brightness temperature to the inverse-Compton limit. This upper limit is consistent with the VLBI measurements (Standke et al. 1996; Krichbaum et al. 2002). However, if we take a smaller value for  $v$  (e.g.  $v < 30$  km s $^{-1}$ ), then the angular size of the lensed components would decrease and their brightness temperatures would correspondingly increase, leading to requiring a higher Doppler factor. In contrast, if the time scale of the event ( $\sim 1$  day) is used to derive the source angular size, we would obtain  $\theta_s \sim 0.08 \mu\text{as}$  ( $H_0 = 100$  km s $^{-1}$  Mpc $^{-1}$ ,  $q_0 = 0.5$ ), and the corresponding brightness temperature would reach  $T_{b,\text{app}} \sim 4.2 \times 10^{18}$  K, as usually encountered in IDV sources.

## 5 CONCLUSIONS

The polarization angle swings of  $180^\circ$  observed in the QSO 1150+812 (Qian et al. 2006) and QSO 0917+624 (this paper) can both be interpreted in terms of focusing–defocusing effects from compact interstellar clouds. Our 4-component models consist of one non-polarized component and three polarized components, two of which are occulted by the cloud almost simultaneously. There is also evidence for the non-polarized component being affected by the cloud. These results indicate the significant role of individual clouds in causing IDVs.

Due to the denser data-sampling during the swing period, the model-fitting results for the swing observed in 0917+624 appear more convincing. The refractive focusing–defocusing effect is a weak scattering process with  $\alpha \sim 1.5$  and the rounded minimum (or ‘occultation’) and the peak at  $\sim 7526$  are well fitted for both component-1 and component-2. However, outside the swing period, the intraday variations could be caused by combined effects due to individual compact clouds and the continuous medium. Usually, dense, compact clouds (like interstellar shocks, see Clegg et al. 1988) can produce focusing–defocusing effects, causing polarization angle swing events when they move across the line of sight to the sources, while the continuous scattering medium causes normal fluctuations in intensity and polarization.

Since the proposed model consists of 4-components and the values chosen for the model-parameters are not unique, future VLBI observations are important to unveil the polarization structure of the source and for checking the required Doppler factor (less than  $\sim 20$ ).

The angular sizes derived for the lensed polarized components are in the range of  $20 - 70 \mu\text{as}$ , depending on the relative velocity  $v$ . For  $\theta_s \gtrsim 40 \mu\text{as}$  the corresponding apparent brightness temperature is  $\lesssim 1.5 \times 10^{13}$  K, therefore a relativistic motion with a Lorentz factor less than 20 is sufficient to conform to the inverse-Compton limit.

The cloud which causes the polarization position angle swing is extraordinarily small: it is only  $\sim 0.01$  AU in size and its electron density is  $\sim 10^2$  cm $^{-3}$ .

Finally we point out that the proposed model is only one of the currently competing models for explaining polarization angle swing events. Comparing the advantages and disadvantages of these different models will be helpful to deepen our understanding the physics of IDV (see Qian & Zhang 2003, 2004).

**Acknowledgements** S. J. Qian acknowledges the hospitality and financial support of the Max-Planck-Institut für Radioastronomie during his two-month visit in 2005.

## References

- Berkhuijsen E. M., Haslam C. G. T., Salter C. J., 1971, *A&A*, 14, 252  
Clegg A. W., Fey A. L., Fiedler R. L., 1996, *ApJ*, 457, L23  
Clegg A. W., Fey A. L., Lazio T. J. W., 1998, *ApJ*, 496, 253  
Clegg A. W., Chernoff D. F., Cordes J. M., 1988, in *Radio Wave Scattering in the Interstellar Medium*, ed. J. M. Cordes, B. J. Rickett, D. C. Backer (New York: AIP), p.174  
Fiedler R. L., Dennison B., Johnston K.J., Hewish A., 1987, *Nature*, 326, 675  
Fiedler R. L., Dennison B., Johnston K. J., Waltman E. B., Simon R. S., 1994, *ApJ*, 430, 581  
Gabuzda D. C., Cawthorne T. V., 2000, *MNRAS*, 319, 1056  
Gabuzda D. C. et al., 1996, *MNRAS*, 283, 759  
Gopal-Krishna, Wiita P. J., 1992, *A&A*, 259, 109  
Heiles C., Jenkins E. B., 1976, *A&A*, 46, 333  
Hu E. M., 1981, *ApJ*, 248, 199  
Kochenov P. Yu., Gabuzda D. C., 1999, in: *BL Lac Phenomenon*, ASP Conference series 159, ed. L. O. Takalo, A. Sillanpää, p.460  
Krichbaum T. P., Kraus A., Fuhrmann L., Cimo G., Witzel A., 2002, *Proc. Astron. Soc. Austr.*, 19, 14  
Marscher A. P., Gear W. K., Trevis J. P., 1992, in *Variability of Blazars*, eds. E. Valtaoja, M. Valtonen, Cambridge University Press, p.85  
Pohl M., Reich W., Krichbaum T. P. et al., 1995, *A&A*, 303, 383  
Qian S. J., Quirrenbach A., Witzel A., Krichbaum T. P., Hummel C. A., Zensus J. A., 1991, *A&A*, 241, 15  
Qian S. J., 1994a, *Acta Astrophys. Sin.*, 4, 333. (English Transl: *Chin. Astron. Astrophys.*, 1995, 19, 69)  
Qian S. J., 1994b, *Acta Astrophys. Sin.*, 35, 362. (English Transl: *Chin. Astron. Astrophys.*, 1995, 19, 267)  
Qian S. J., Britzen S., Witzel A. et al., 1995, *A&A*, 295, 47  
Qian S. J., Witzel A., Kraus A., Krichbaum T. P., Zensus J. A., 2001a, *A&A*, 367, 770  
Qian S. J., Kraus A., Krichbaum T. P., Witzel A., Zensus J. A., 2001b, *Ap&SS*, 278, 119  
Qian S. J., Kraus A., Zhang X. Z., Krichbaum T. P., Witzel A., Zensus J. A., 2002, *Chin. J. Astron. Astrophys. (ChJAA)*, 2, 325  
Qian S. J., Zhang X. Z., 2003, *Chin. J. Astron. Astrophys. (ChJAA)*, 3, 75  
Qian S. J., Zhang X. Z., 2004, *Chin. J. Astron. Astrophys. (ChJAA)*, 4, 37  
Qian S. J., Krichbaum T. P., Zhang X. Z. et al., 2006, *Chin. J. Astron. Astrophys. (ChJAA)*, 6, 1  
Quirrenbach A., Witzel A., Qian S. J., Krichbaum T. P., Hummel C. A., Alberti A., 1989, *A&A*, 226, L1  
Quirrenbach A., Kraus A., Witzel A. et al., 2000, *A&A*, 354, 380 (and *A&AS* 141, 221)  
Rickett B. J., Quirrenbach A., Wegner R., Krichbaum T. P., Witzel A., 1995, *A&A*, 293, 479  
Rickett B., Kedziora-Chudzycer L., Jauncey D. L., 2002, *PASA*, 19, 106  
Simonetti H. J., 1991, *A&A*, 250, L1  
Standke K. J., Quirrenbach A., Krichbaum T. P. et al., 1996, *A&A*, 306, 27  
Wagner S., Witzel A., 1995, *ARA&A*, 33, 163  
Wambsganss J., Schneider P., Quirrenbach A., Witzel A., 1989, *A&A*, 224, L9.  
Witzel A., 1992, in: *Physics of Active Galactic Nuclei*, ed. W. J. Duschl, S. J. Wagner, Springer Heidelberg, p.484